2006 Annual Society for Experimental Mechanics (SEM) Conference
St. Louis, Missouri; June 4-7, 2006
Approved for Public Release, Distribution Unlimited.

Fatigue and Stress Monitoring with Magnetic Sensor Arrays

Neil Goldfine, David Grundy, Andrew Washabaugh, Chris Craven,
Volker Weiss, Vladimir Zilberstein
JENTEK Sensors, Inc., 110-1 Clematis Avenue, Waltham, MA 02453-7013
Tel: 781-642-9666; Fax: 781-642-7525; Email: jentek@shore.net

ABSTRACT

Background and selected applications of conformable eddy current sensor networks for monitoring fatigue damage in complex geometry regions of specimens, components and structures are presented. Also, capability to use the same sensors to monitor stress in ferromagnetic materials is described. These eddy current sensors, called MWM®-Arrays, use model-based multivariate inversion methods to provide reliable early detection and monitoring of fatigue cracks and real-time monitoring of stress through paint or coatings. Proven capabilities are illustrated by results for aluminum alloy, titanium alloy, and high-strength steel fatigue specimens, with MWM-Arrays mounted inside holes and on other cylindrical surfaces. Linear and circular MWM configurations (MWM-Rosettes) also provide the capability to detect and monitor fatigue cracks in embedded (between layers) sensor formats and with sensors placed under bolt heads as "smart washers." This paper describes implementations of this capability for aircraft focused applications, including past and ongoing coupon, sub-component, component and full-scale aircraft fatigue tests as well as for structural health monitoring.

INTRODUCTION

Fatigue monitoring using Meandering Winding Magnetometer (MWM®) sensor arrays (MWM-Arrays) with model-based multivariate inversion methods [1] was first introduced in the mid 1990's [2]. The method is based on the realization that mechanical fatigue damage affects the effective electromagnetic properties of the material, e.g., electrical conductivity and magnetic permeability as measured by the MWM-Array sensors. Changes in the effective properties associated with fatigue crack initiation and propagation occur over a scale, comparable to the dimensional sensitivity of MWM-Array sensors. Excellent progress in fatigue monitoring with these sensors has been achieved over the last ten years [3-8].

Recent focus has been on detection of cracks shorter than 250 μm (length at the surface) in aluminum and titanium alloys. In fatigue tests with vintage aluminum alloys, where cracks tend to initiate at inclusions, clusters of cracks with no single crack exceeding 50 μm have been detected, using electrical conductivity measurements. Early fatigue damage detection using magnetic permeability measurements has been demonstrated for steels, e.g., Type 304 stainless steel and 4340 low-alloy steel.

These capabilities open new opportunities for fatigue test monitoring, particularly when there is a need to determine fatigue life to a certain damage level or a specified "small" crack size. This is often needed in fatigue testing of components and substructures, as well as in full scale fatigue tests. This capability is expected to be used in tests of fatigue specimens to separate the "initiation" and propagation stages.

MWM-Arrays also provide the capability to monitor stresses [9]. Stress measurements with MWM-Arrays have a number of advantages over existing methods. Some of these advantages include the capability to measure stresses through an air gap, through a coating, or through a non-ferromagnetic layer.

This paper provides a brief review of fatigue monitoring and stress monitoring capabilities using results of selected tests with MWM-Arrays mounted on the test articles as well as with scanning MWM-Arrays.

MWM-ARRAY SENSORS

Several examples of scanning and permanently mountable MWM-Array eddy current sensors and selected applications of these sensors are shown in Figures 1 and 2. Each sensor has one drive winding, consisting of one, two or several rectangular loops. The sensing elements are simple rectangular coils. The transimpedance (sensing element voltage/drive current) is measured for each sensing element. Each of these sensor designs are covered by issued or pending U.S. patents, including but not limited to U.S. patent #5,015,951, RE36,986, #5,453,689, #5,629,621, #5,793,206, #5,966,011, #6,188,218, #6,252,398, #6,351,120, #6,420,867, #6,784,662 and #6,952,095.

These sensors are carefully designed to enable modeling from basic physical principles and to minimize unmodeled contributions to the sensor response. Each sensing element response at one or more input current frequencies is used by a multivariate inversion routine to determine the absolute property values (electrical conductivity or magnetic permeability) at the location of the sensing element on the test specimen or component. In this inversion, databases of precomputed sensor responses are used with a table look-up algorithm to convert complex impedance data into two or more unknown property estimates at each sensing element. In a permanently mounted mode, data is taken at prescribed times. In a scanning mode, data is taken at each sensing element as it traverses a part to produce an image of each unknown property of interest. Higher frequencies provide information about near surface properties, and lower frequencies provide information about subsurface properties.

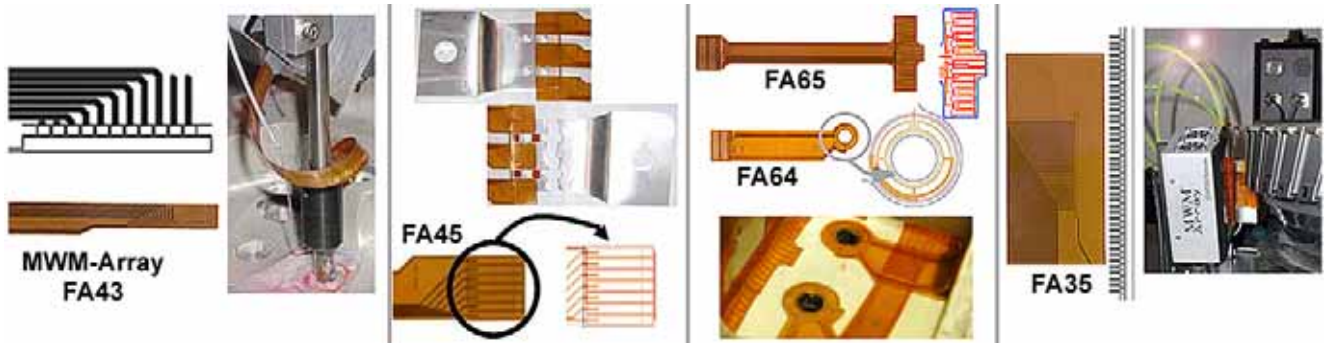

(a) (b) (c) (d) (e)

Figure 1. Examples of scanning, embedded and surface mountable MWM-Arrays: (a) scanning MWM-Array for damage detection in difficult-to-access locations; (b) bolt hole inspection for fatigue cracks; (c) embedded sensors for multisite damage detection/monitoring; (d) MWM-Rosette under fasteners (“smart washer”) for buried crack detection and linear MWM-Arrays for surface crack detection in difficult-to-access locations; and (e) inspection/ imaging of fatigue cracks in engine disk slots.

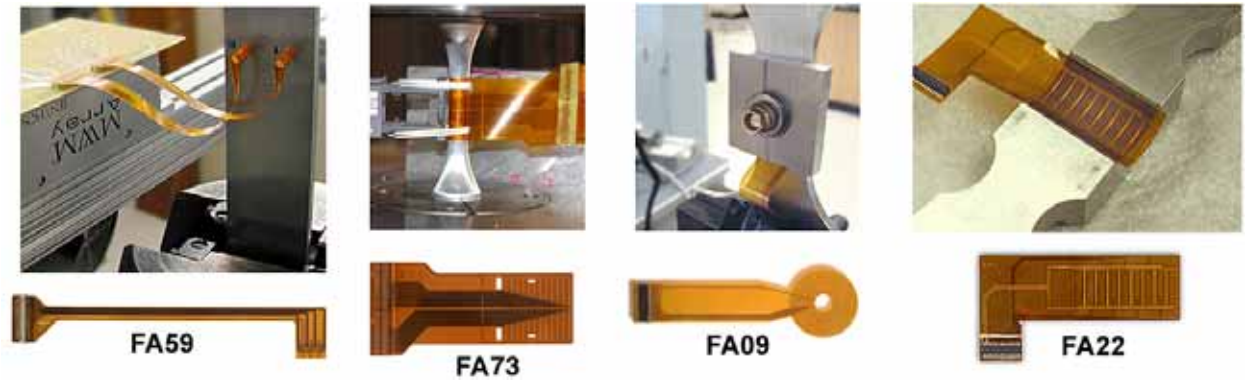

(a) (b) (c) (d)

Figure 2. Additional examples of MWM-Array configurations: (a) fatigue monitoring inside holes; (b) MWM-Array monitoring of strain-life test; (c) fatigue monitoring with an embedded MWM-Rosette; and (d) 4340 low alloy steel early fatigue damage detection/monitoring.

MWM-ARRAY EARLY DAMAGE DETECTION CAPABILITY

Early Stage Fatigue Damage Monitoring in 4340 Low Alloy Steel

JENTEK has demonstrated the capability to detect and monitor early stage fatigue damage in cyclically loaded, shot peened, high-strength steel components via magnetic permeability measurements. The permeability measurements can be performed either at preselected intervals during the test using permanently mounted MWM-Arrays or intermittently, when the test is interrupted, with scanning MWM-Arrays. The results obtained to date suggest that MWM-Array permeability measurements can provide early detection of fatigue damage in steels *before* conventional methods can detect any changes. This has been demonstrated to be particularly significant in the presence of high compressive stresses introduced by shot peening. Note that many critical landing gear and rotorcraft components are shot peened to improve fatigue resistance.

Results of the MWM permeability measurements made during a fatigue test of the shot peened specimen are presented in Figure 3 together with the FASTRAN predicted crack growth curve[1]. The increase in permeability such as shown in Figure 3 (bottom left) captures changes occurring in steel components during cyclic loading that causes fatigue damage. In this test, after the first 15,000 cycles, the sensing elements in the center of the specimen (the higher stress area) detected significant changes in permeability. These permeability changes proved to be indicative of early stage (pre-crack) fatigue damage, as verified by fractography.

Figure 4 (left) shows the permeability image obtained with a scanning MWM-Array on the same 4340 specimen after the test was stopped. This image shows the distribution of fatigue damage in the high-stress area of the specimen and reveals two adjacent zones within the image with a higher permeability. The zone on the left contains two spots with the highest permeability, corresponding, as verified by fractography, to two cracks. The zone of higher permeability on the right did not have any cracks, and reveals precrack fatigue damage. This precrack damage is not detectable by any other practical on-aircraft sensing method.

Examination of the fatigue specimen in a scanning electron microscope (prior to fractography) detected only a few relatively small cracks, e.g., 50 to 200 µm long (0.002 in. to 0.008 in.), associated with the left zone of higher permeability. Fractography, however, revealed significantly longer cracks (Figure 4, lower right). For the **same** specimen, conventional eddy current, ultrasonic testing and magnetic particle inspection (ET, UT, MPI), performed by an OEM, failed to provide any indications of cracks. The inability of conventional NDT to detect cracks reliably in shot peened components is a major concern, as these techniques are broadly used by DoD and commercial airlines to inspect critical shot-peened components.

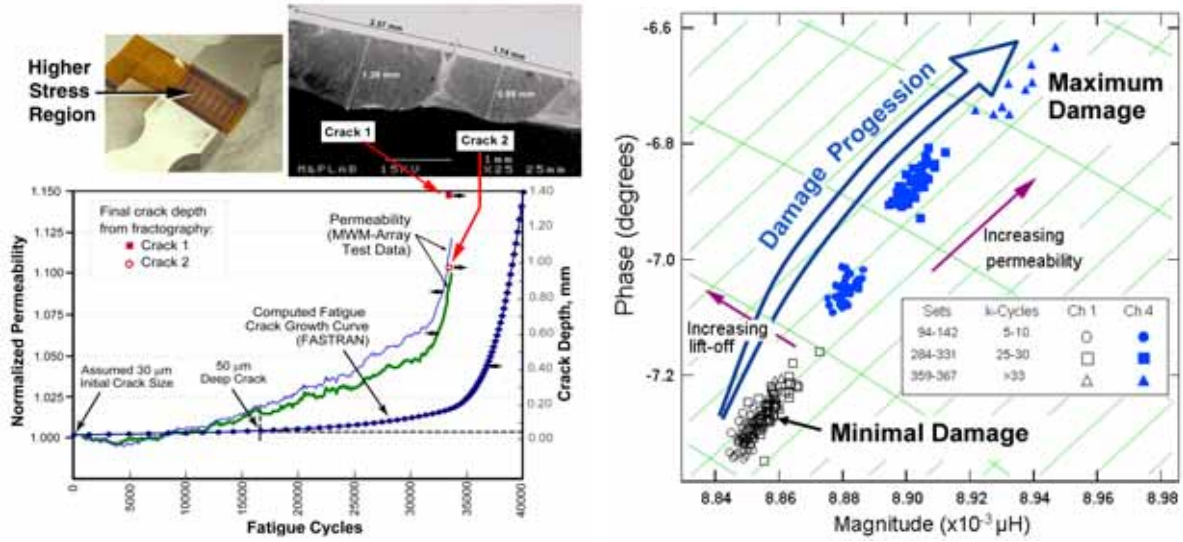

Figure 3. (Left) MWM-Array measured magnetic permeability curves and fatigue crack growth curve (from FASTRAN analysis). (Right) Detail of the measurement grid (precomputed sensor responses) indicating response of MWM-Array Channels 1 and 4 within selected ranges of load cycles (Channel 1 was monitoring a lower stress location, while Channel 4 was monitoring the highest stress location). The fatigue damage progression in 4340 steel is reflected in the gradual increase of MWM-Array measured magnetic permeability.

[1] FASTRAN analysis was performed by Prof. J. Newman.

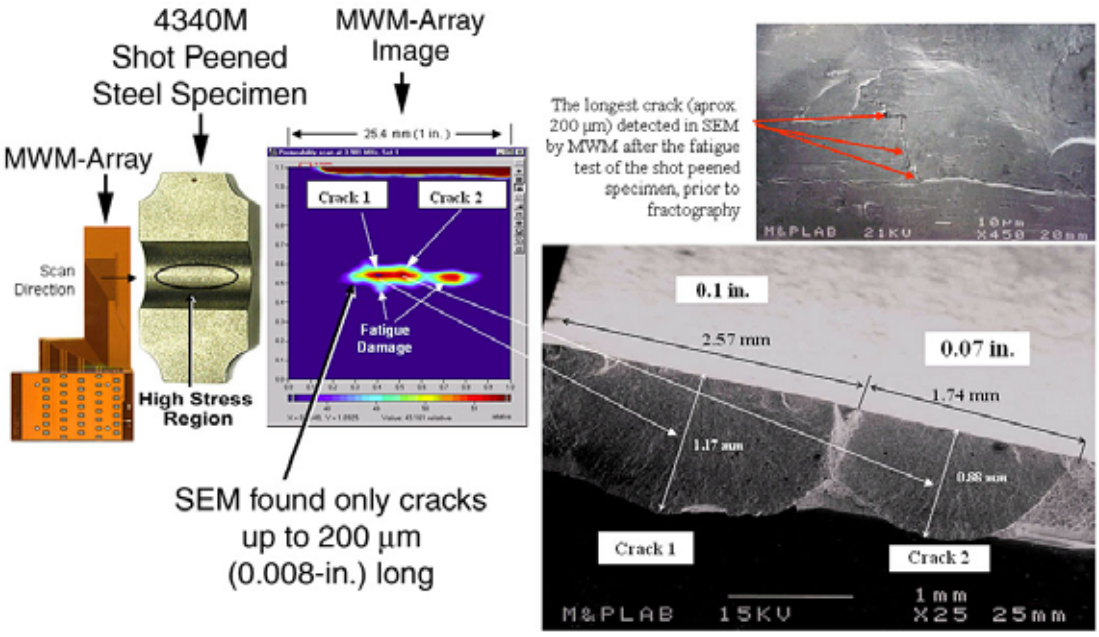

Figure 4. Fractography revealed two coalesced cracks significantly larger than could be inferred from scanning electron microscope (SEM) observations. Note that traditional NDE, performed by reputable 3rd party, Level III inspectors, failed to detect these cracks in the shot peened steel.

Detection and Monitoring of Early Stage Fatigue Damage in Austenitic Stainless Steel

In work conducted in the mid-90s, under JENTEK IR&D and Department of Energy funding JENTEK demonstrated that MWM sensors are capable of detecting very early stage fatigue damage (**prior to formation of cracks**) in materials that undergo strain-induced phase transformations. More recently, flat dog-bone Type 304 stainless steel specimens were examined with an imaging MWM-Array. Figure 5 shows MWM-Array measured permeability images for these specimens. One of the specimens was never fatigue tested and was still fully austenitic and, thus, nonmagnetic (relative permeability, $\mu_r = 1$). The other specimen (tested to 88% of fatigue life) was in a similar fully austenitic condition prior to the fatigue test. However, cyclic loading results in magnetic permeability changes indicating fatigue damage as shown in the MWM permeability image in Figure 5 (right). These changes for Series 300 austenitic stainless steels are associated with strain-induced martensite that forms during cyclic loading at ambient temperature. The fatigue damage region in the image shown in Figure 5 (right) is well defined by the higher magnetic permeability as measured by the MWM-Array. The image also reveals two localized zones (toward the left end of the gage section) of somewhat higher permeability compared to the remainder of the gage section of the specimen, except for one dark spot (corresponding to a small indentation) of significantly higher permeability. The localized zones of somewhat higher permeability are likely sites of future crack initiation.

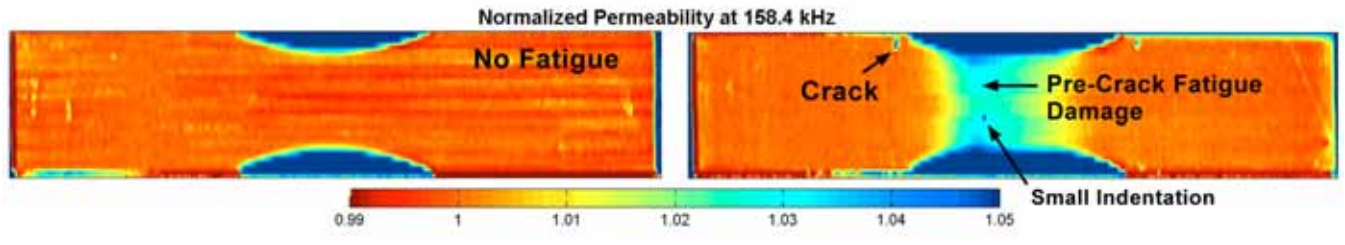

Figure 5. Magnetic permeability images generated with an MWM-Array for (left) a control specimen that has not been subject to fatigue testing and (right) a specimen tested to 88% of fatigue life.

The MWM capability to accurately perform bidirectional magnetic permeability measurements can further enhance detection of precrack fatigue damage in Type 304 stainless steel. Figure 6 illustrates this capability to detect fatigue damage in tension-tension specimens with results generally similar to the four-point bending specimen results shown in Figure 5. Again, fatigue damage is reflected by the magnetic susceptibility increase (note: magnetic susceptibility, $\chi = \mu_r - 1$, where μ_r is the relative permeability); this increase indicates formation of martensite due to plastic deformation associated with cyclic loading.

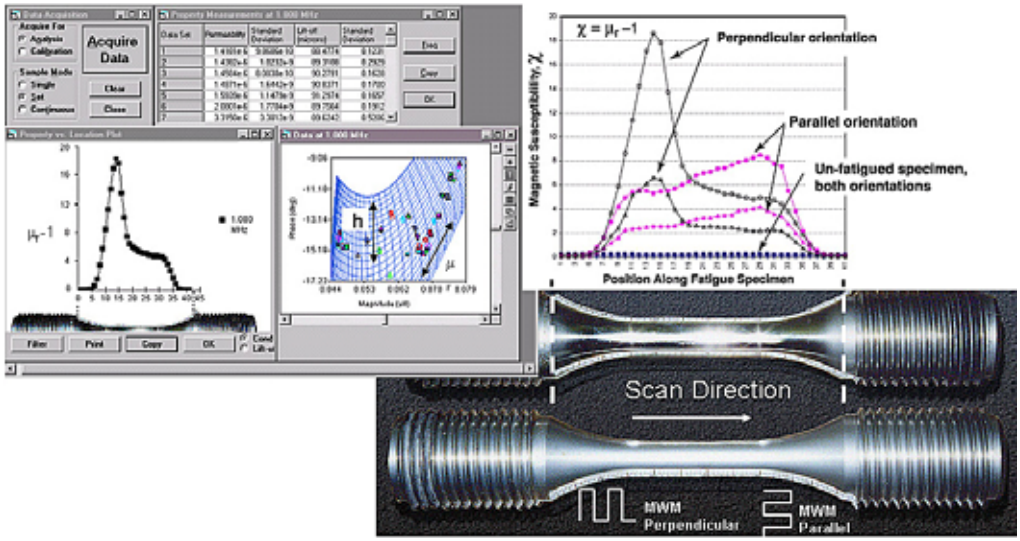

Figure 6. Detection of fatigue damage in Type 304 stainless steel specimens using GridStation software module for characterization of slightly magnetizable material. Specimens provided by Siemens.

Early Stage Fatigue Damage Detection in 7075-T651 Aluminum

In an ongoing program being sponsored by DARPA, as a subcontractor to Northrop Grumman, JENTEK demonstrated the capability to (1) generate correlation relationships between MWM-Array monitored electrical conductivity and small crack lengths (for lengths of 0.13 to 2 mm (0.005 in to 0.2 in.), (2) to detect small cracks with high probability for cracks greater than 64 µm (0.0025 in.) depth by 0.13 µm (0.005 in.) length and about 50% probability for 25 µm (0.001 in.) depth by 50 µm (0.002 in.) length that form in clusters, and (3) to support prognostics model validation and calibration for early stage fatigue damage detection. Depending on the definition of precrack damage, this capability demonstration reaches into the “precrack” regime, well below the threshold that many experts previously defined as crack initiation. This adaptation of the MWM-Array sensor network was performed under a recently completed NAVAIR SBIR, and the FA59 MWM-Array sensor development was performed under JENTEK IR&D.

FA59 MWM-Arrays were mounted inside two holes in tensile fatigue specimens as shown in the configuration in Figure 2(a). This MWM-Array has three rows of sensing elements, which were oriented in the hole to cover the 3 o’clock, 9 o’clock and 12 o’clock positions, as indicated in Figure 7(a). The loading direction was expected to generate cracks at the 3 o’clock and 9 o’clock positions. Numerous coupon tests were performed and stopped for destructive testing. Figures 7(b) and (c) show the MWM-Array conductivity response and the conversion of this response to crack size estimates for one example coupon test. Figure 7(d) shows the correlation data used to determine the sensitivity and derive the correlation function relating individual sensing element conductivity to a crack size estimate in real-time.

Figure 7(c) covers the range of crack sizes, from 100 µm (0.004 in.) up to 2500 µm (0.100 in.). The SEM photo shown in Figure 7(e) reveals a number of cracks that have lengths in the range of 100 µm (0.004 in.) to 250 µm (0.010 in.) and that have just begun coalescing, prior to the formation of a dominant crack.

Note that dozens of fatigue tests were performed under this program using MWM-Array sensors to monitor fatigue damage inside the holes, and all tests were stopped when the damage state was in the desired range. To our

knowledge, there is no other technology that permits such reliable, autonomous, and convenient control over fatigue tests when it is desired to stop the test at early stages of damage.

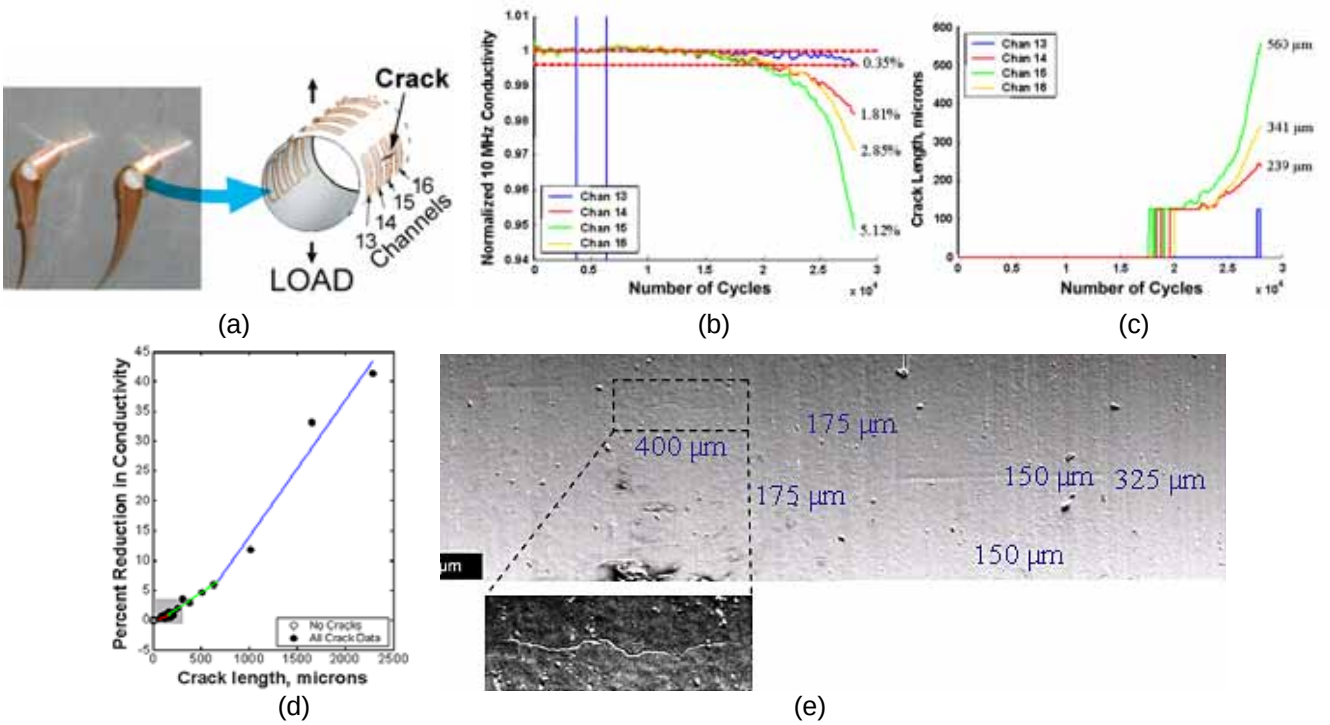

(a) (b) (c)

(d) (e)

Figure 7. (a) MWM-Array sensing elements were located at the 3 o'clock, 9 o'clock, and 12 o'clock positions; (b) local normalized MWM-Array measured conductivity vs. number of cycles, (c) crack size estimates based on local conductivity drop, (d) the correlation developed between crack length and percent reduction in conductivity, which was generated from a number of destructively examined specimens; (d) SEM image of one side of a representative specimen.

Monitoring Fatigue Damage in Titanium Alloy Specimens

Annealed Ti-6Al-4V samples were cyclically loaded to generate fatigue cracks. Two FA75 MWM-Array sensors were used to monitor each test, one mounted in each of the two holes in the fatigue specimen. The sensors were curled up, inserted into the holes, and pressed against the surface so that the sensing elements were positioned at the 3 and 9 o'clock positions within the hole. The specimens underwent tension-tension fatigue where the maximum load was 20,000 lbs, and the R value was 0.1. The test was performed at a cycling frequency of 3 Hz.

As the fatigue test progressed, the MWM-Arrays continuously monitored local changes in effective conductivity that are associated with the formation and growth of cracks. These measurements were acquired and displayed in real-time. Results for a specimen that was run to partial failure are shown in Figure 8. In this specimen, no damage was detected in the top hole (monitored by Channels 13-18 on the left side and Channels 19-24 on the right side), as well as in the bottom hole on the right side (monitored by Channels 7-12). The crack that formed in the lower hole on the left side was monitored from initiation to ligament failure by Channels 1-6. As shown in these results, the crack first formed at the edge of the specimen monitored by Channel 6, then progressed across Channels 5,4,3,2 and 1 before finally breaking through the ligament. Photographs of the specimen as well as MWM-Array response plots for this specimen are shown in Figure 8.

This demonstration illustrates the importance of on-board sensors for monitoring fatigue damage. Note that for the same specimen, geometry and material and even for identical equally stressed geometric features in the same specimen, variations in the number of cycles to crack initiation can be huge. **Thus, prognostics models will be most valuable when combined with early fatigue damage detection sensors.**

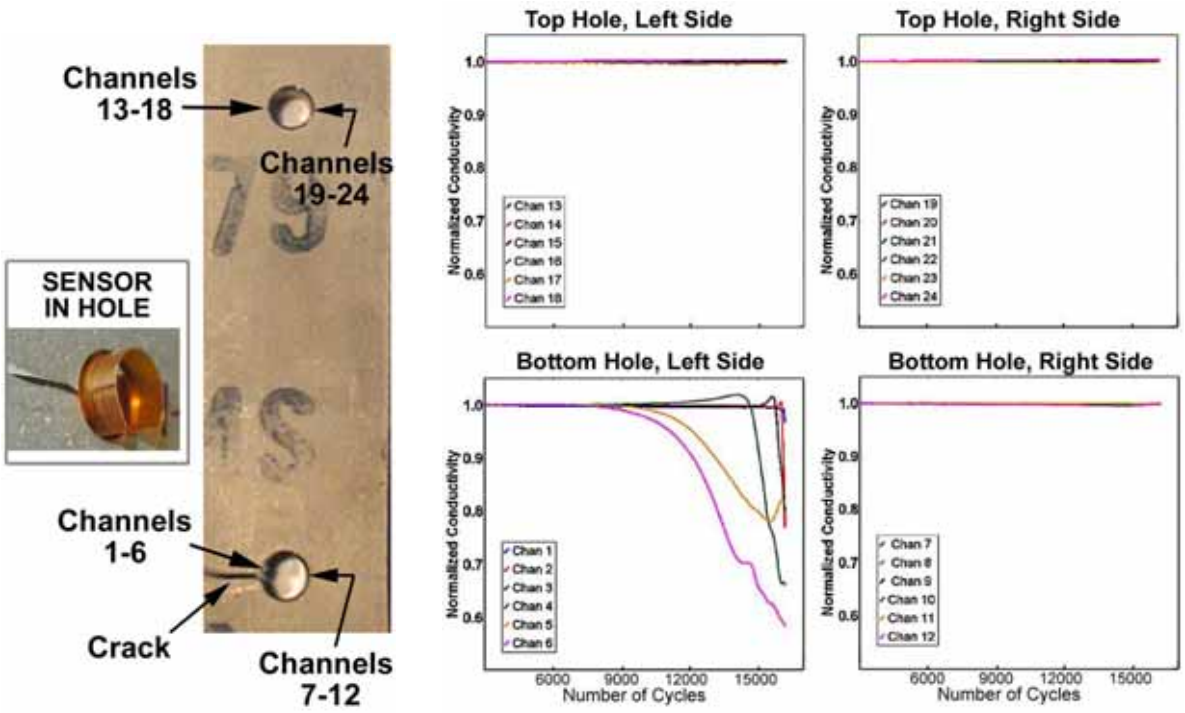

Figure 8. MWM-Array response for a Ti-6Al-4V fatigue specimen that was tested to partial failure. Two FA75 sensors monitored this test, each with 12 channels. The test ran to 16,264 cycles before the specimen broke through the left ligament on the bottom hole (channels 1-6).

Multisite Fatigue Test Monitoring

In fatigue tests performed for the Air Force under a subcontract to Lockheed Martin, ten-hole lap-joint specimens with embedded MWM-Arrays mounted between the holes in the lower and upper rows were used; see Figures 9(a) and 9(b). Figure 9(c) shows the equipment set-up with the specimen in the load frame and the JENTEK 37-channel probe. A variety of precrack configurations were tested with larger ("primary") precracks at the center hole and smaller ("secondary") precracks at the other holes. The crack tip progression data are shown in Figure 10. The lines indicate progression of crack tips from one hole towards another as a function of number of cycles. The MWM-Arrays successfully monitored crack growth throughout the test with the sensors embedded at the buried interface between the metal plates. The sensors survived the test in which the specimen failed. **These sensors can be used for multiple fatigue tests. In fact, no sensors failed in subsequent tests, i.e., the same sensors were reused in multiple tests – lasting several coupon lifetimes [8].**

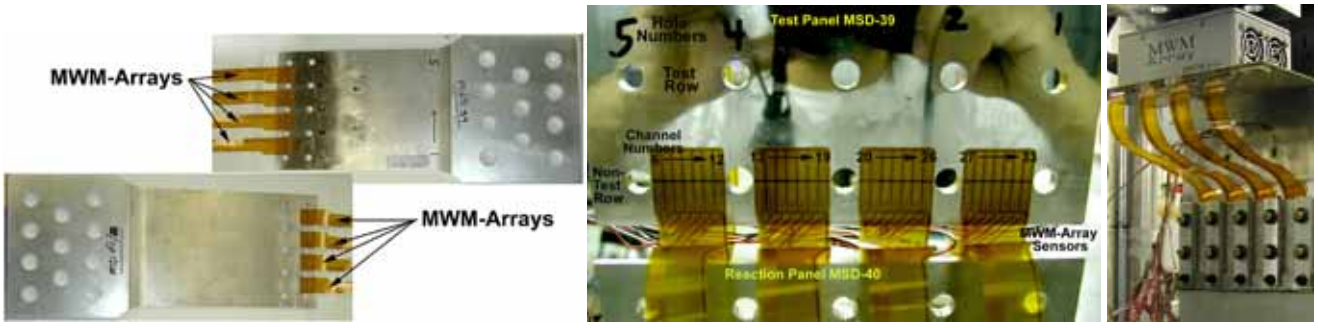

(a) (b) (c)

Figure 9. (a) MWM-Arrays mounted along both rows of fastener holes. (b) The ten-hole specimen with embedded MWM-Arrays shown prior to bolting up. (c) The ten-hole specimen mounted in the load frame.

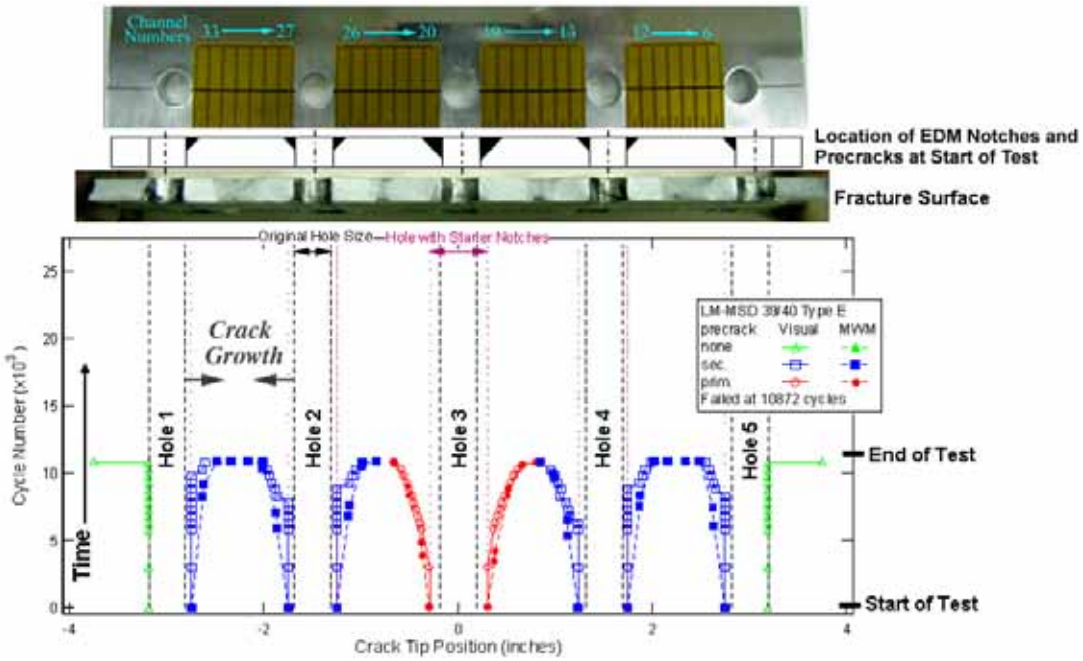

Figure 10. Representative multiple crack growth monitoring data. The specimen had primary (prim.) precracks at Hole 3 and secondary (sec.) precracks at the other holes.

Strain Life Testing

MWM-Arrays can be used for detection of fatigue damage in dogbone and hourglass fatigue specimens such as those used for strain-controlled fatigue testing. Strain-controlled fatigue tests per ASTM E606 are performed "at least until failure and preferably until fracture" [11]. There is an interest in determining the number of cycles required to "initiate" a crack, for example a 0.010-in. long crack. For preliminary tests, performed under DARPA funding/subcontract to Northrop Grumman, a standard MWM-Array was used, see Figure 11(a) and (b). In these constant strain amplitude, fully reversed fatigue tests of round-bar hourglass specimens, an FA23 MWM-Array sensor was wrapped around the test section of the specimen. When cracks form under the footprint of the sensor, a reduction in the effective conductivity and an increase in effective lift-off are measured by this array (see Figure 11). For this sensor and material, a readily measured 0.075 percent decrease in the effective conductivity indicates the presence of 0.010-in. long cracks. New MWM-Arrays, developed under JENTEK IR&D, as shown in Figure 11(c) and Figure 2(b), can provide a nearly 100 percent coverage of the test section of the specimen with adequate sensitivity and signal-to-noise ratio.

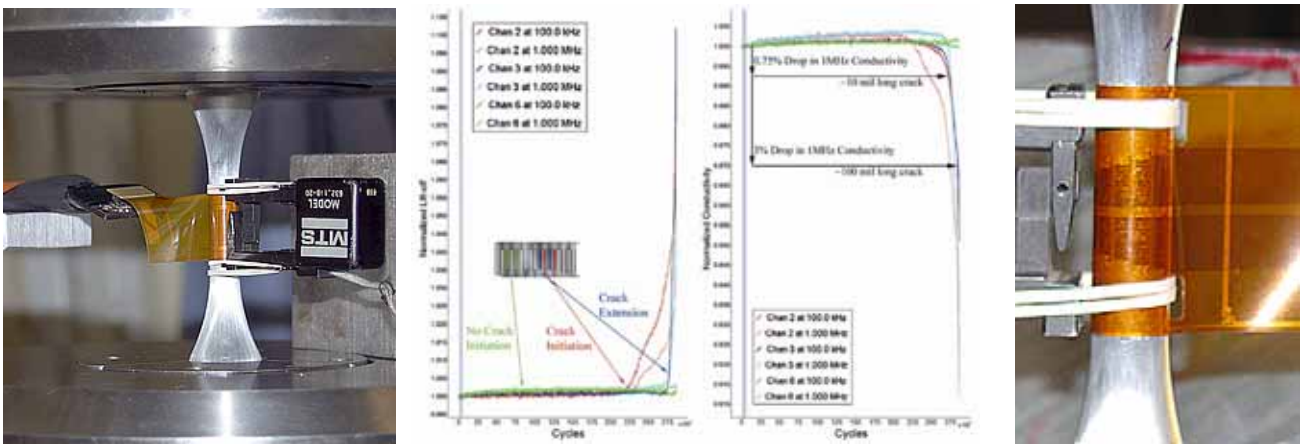

(a) (b) (c)

Figure 11. (a) Strain life testing with an FA23 sensor performed at Northrop Grumman. (b) MWM-Array results for one of the specimens, and (c) modified MWM-Array design to provide improved gage region coverage.

Fatigue Crack Specimen Fabrication

JENTEK has developed methods for fabrication of fatigue crack specimens with made-to-order cracks in representative coupon or component geometries. MWM-Arrays are mounted on a fatigue specimen prior to loading and are monitored during cycling. The arrays track crack initiation and growth and permit the test to be terminated when the desired crack size is reached.

Figure 12 (a) illustrates the mounting location of two FA51 MWM-Arrays on an IN718 punched slot specimen. The specimen was mounted in a four-point bend test fixture that concentrated stress at the slot ends, where the sensors were mounted. This work was performed for NASA LaRC. Figure 12(b) provides the sensor output for the arrays mounted on the left and right sides of the slot. Crack growth across the various sensing channels was monitored as changes in effective conductivity. Prior to this, the sensor response had been simulated for a crack progressing across the volume of material under the MWM-Array. The simulation results were used to interpret sensor output to obtain an estimated crack length. As was predicted by the simulations, the elements closest to the slot (Channels 1 and 4) showed a continuous decrease in effective conductivity as the cracks grew across them. As the cracks approached the second sensing elements (Channels 2 and 5), the effective conductivity measured by this channel first increased, then decreased. Some of the specimens produced were examined by SEM and determined to be in good agreement with the predicted crack lengths. Using this method, we successfully produced specimens with cracks from 0.127 to 1.27 mm (0.005 in. to 0.050 in.) long, emanating from the apexes of the slots, which was the goal of the program [9].

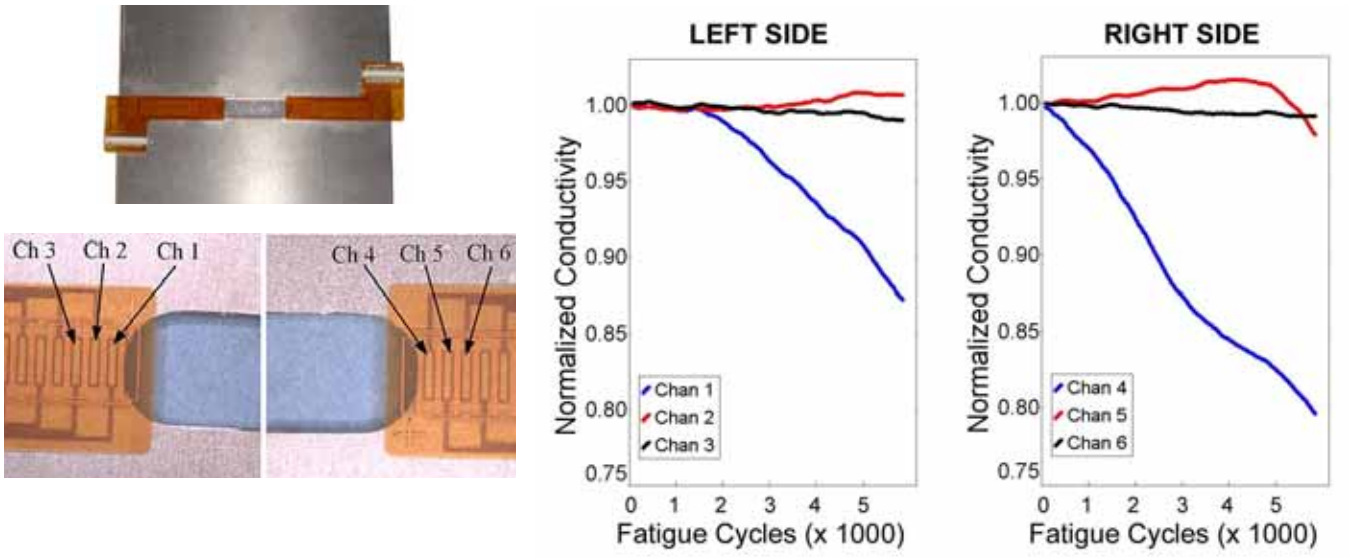

(a) (b)

Figure 12. (a) Photographs illustrating how the two FA51 MWM-Arrays were mounted on each specimen prior to the fatigue test. Sensors were mounted on the burred (punch exit) side of the specimen, and remained on the specimen during the testing. (b) Sensor response during the fatigue test.

Buried Damage Detection with Deep Penetration Permanently Mounted MWM-Arrays

MWM-Arrays provide detection of buried cracks. This has been demonstrated in laboratory tests with MWM-Rosettes mounted around holes (Figure 13) on external surfaces, between layers, and on internal surfaces. The schematic at the left in Figure 13 conceptually shows placement of an MWM-Rosette around a fastener on an external surface (for fatigue test monitoring). The plots in Figure 13 show results for a fatigue test of a specimen with two holes, together with the fractography results. This test was performed by JENTEK at Northrop Grumman under DARPA funding. This capability has a significant potential for both full-scale fatigue monitoring and structural health monitoring on aircraft structures. Figure 14(a) shows an example of how such sensors are placed under a washer. Alternatively, the sensors can become a part of the "smart" washer, as shown schematically in Figure 14(b). This concept is disclosed in U.S. patent # 6,952,095 B1.

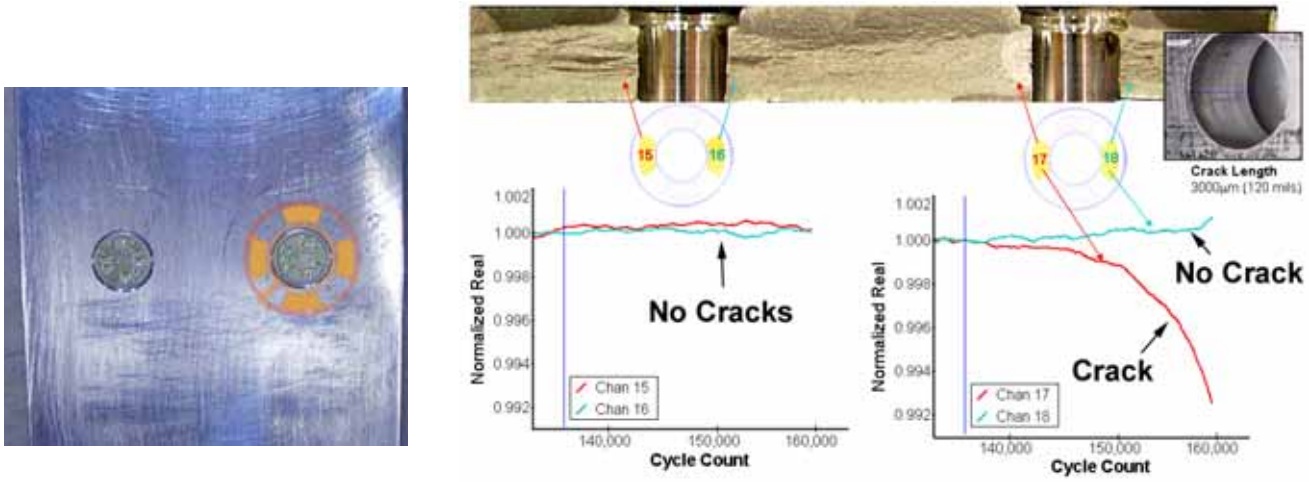

(a) (b)

Figure 13. (a) Schematic of an MWM-Array FA80 sensor superimposed on a photograph of an aluminum fatigue specimen with fasteners. (b) Test results showing the detection of buried cracks formed during a fatigue test of an Al7075 specimen with fasteners in the holes. Also shown are photographs of a fatigue crack on a fracture face and of the crack on the internal surface of the hole prior to fractography.

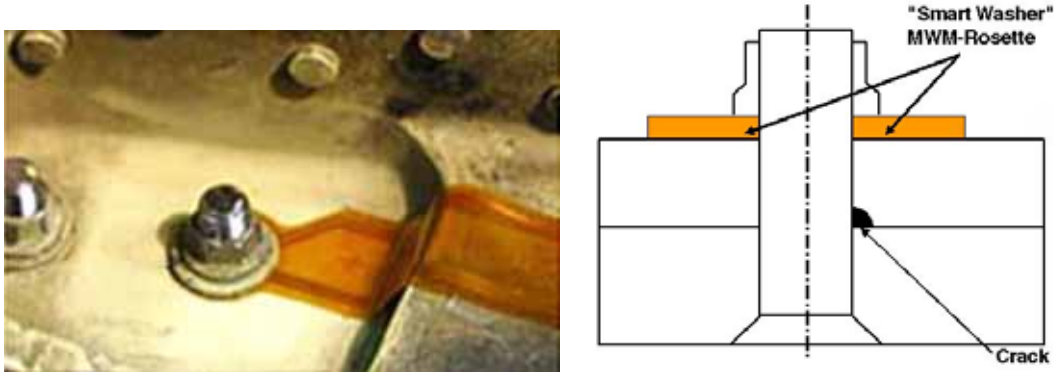

(a) (b)

Figure 14. (a) MWM-Arrays mounted to monitor fatigue cracks at bolt holes on an aircraft structure; (b) example fastener geometry with sensor location.

Aircraft Full-Scale Fatigue Test Monitoring

Past and ongoing full scale fatigue tests with MWM-Array fatigue monitoring networks have not only demonstrated robustness of the MWM-Array sensors for applications in tests, but also serve to support upcoming on-board structural health monitoring applications. Full-scale fatigue monitoring of critical structural members, using surface mounted MWM-Arrays was first demonstrated in 1998 jointly with Lockheed Martin on P-3 aircraft [12] in difficult-to-access locations. Since then, MWM-Arrays have been used in a number of full scale fatigue tests.

Magnetic Stress Gage™ Networks for Stress Monitoring

Previously, a capability to measure stresses via magnetic permeability measurements using MWM sensors was demonstrated [9]. This capability can be used for dynamic stress monitoring. In Figures 15, dynamic stress monitoring with a network of MWM sensors acting as Magnetic Stress Gages is illustrated for steel, see Figure 15(a) and a nonferrous alloy with a thin (0.0005 in thick) stress sensitive magnetic layer applied to the surface - Figure 15(b) (U.S. patents issued and pending). In both cases, MWM sensors are mounted on the front and back

of the metallic strips. When the inverted pendulum is set into motion, the MWM sensors detect the alternating tensile and compressive stresses being experienced by the strips and correctly indicate their phase relationship.

The capability to provide dynamic stress monitoring using surface mounted MWM sensors and arrays has been demonstrated not only for surface stress monitoring, but also for stress monitoring through intervening metal layers and at buried interfaces using projected magnetic fields. [13]

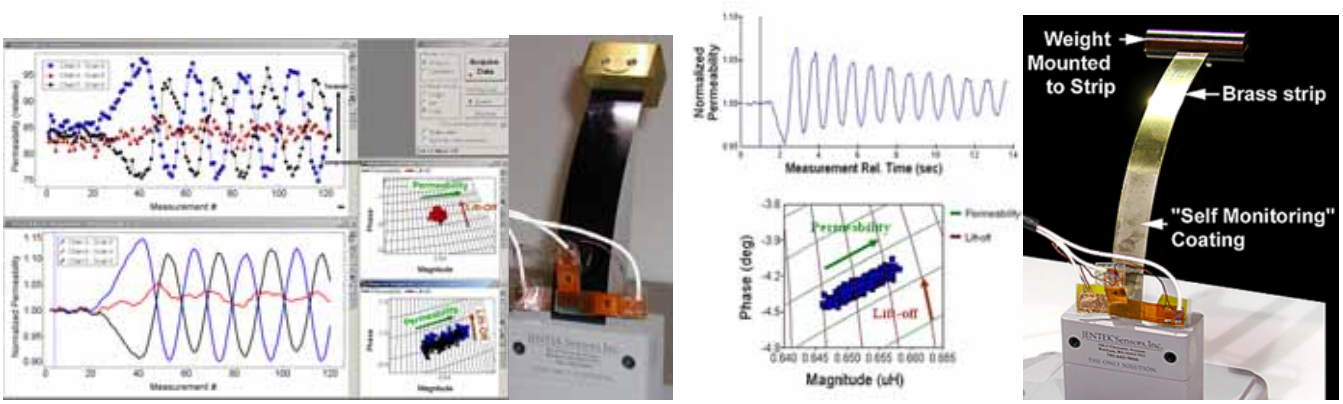

(a) (b)

Figure 15. (a) Demonstration of dynamic stress monitoring in a steel strip using networked MWM-Array sensors. (b) Demonstration of dynamic stress monitoring in a nonferrous alloy strip using networked self-monitoring MWM-Array sensors, with a stress sensitive magnetic coating (i.e., a self-monitoring coating).

Overload Detection

As part of an OEM component test, independent applied load monitoring and overload detection was demonstrated (see Figure 16). The MWM-Array designated Sensor 2 provides applied load monitoring, while the MWM-Array designated Sensor 3 is sensitive only to the relaxation of residual stress associated with an overload event (e.g., a hard landing for a landing gear component) since it measures permeability changes in the direction perpendicular to the applied load.

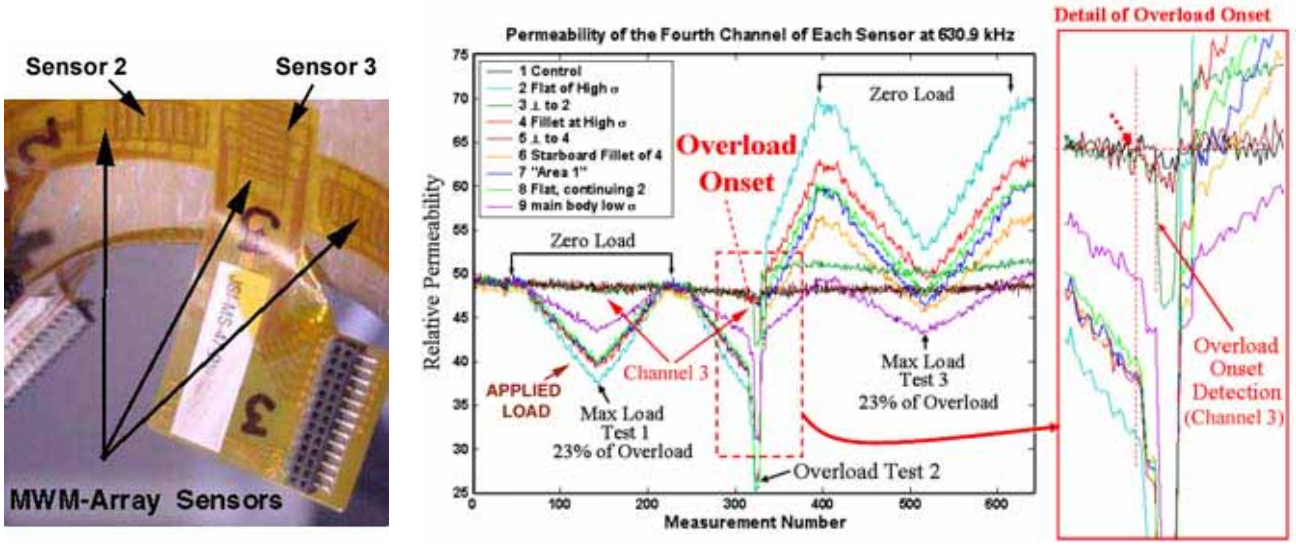

Figure 16. Left, photograph of landing gear component with MWM-Arrays mounted on a critical surface. Right, MWM data showing independent stress monitoring and overload detection due to relaxation of residual stress. Note the indicated green channel corresponds to the sensor which detects the overload event and does not vary with applied loads. This was part of an OEM test.

CONCLUSIONS

The need for practical fatigue and stress sensor technology is pervasive. The sensors described in this paper will provide enhanced diagnostics and damage progression prediction capabilities and new capabilities for load monitoring of structures and dynamic components.

REFERENCES

[1] Goldfine, N., "Magnetometers for Improved Materials Characterization in Aerospace Applications," ASNT *Materials Evaluation*, Vol. 51, No. 3, p. 396-405; March 1993.

[2] Goldfine, N., Clark, D., "Introduction to the Meandering Winding Magnetometer (MWM) and the Grid Measurement Approach," SPIE Nondestructive Evaluation Techniques for Aging Infrastructure and Manufacturing, Scottsdale, Arizona; Dec., 1996. *SPIE Proceedings*, Vol. 2944, 1996. p186-192.

[3] Zilberstein, V., Grundy, D., Goldfine N., Abramovici, E., Yentzer, T., "Early detection and monitoring of fatigue in high strength steels with MWM-Arrays," *International Journal of Fatigue*, Vol. 27/10-12, pp 1644-1652, Fatigue Damage of Structural Materials V. December 2005.

[4] Goldfine, N., Zilberstein, V., Washabaugh, A., Weiss, V., Grundy, D., "The Use of Fatigue Monitoring MWM-Arrays in Production of NDI Standards with Real Fatigue Cracks for Reliability Studies", 16th World Conference on Nondestructive Testing, Montreal, Canada; August-September, 2004.

[5] Goldfine, N., Zilberstein, V., A. Washabaugh, D. Schlicker, I. Shay, D. Grundy, "Eddy Current Sensor Networks for Aircraft Fatigue Monitoring," ASNT *Materials Evaluation*, Vol. 61, No. 7, July 2003, pp. 852-859.

[6] Zilberstein, V., Walrath, K., Grundy, D., Schlicker, D., Goldfine, N., Abramovici, E., Yentzer, T., "MWM Eddy-Current Arrays for Crack Initiation and Growth Monitoring," *International Journal of Fatigue*, Volume 25, 2003, pp. 1147-1155.

[7] Zilberstein V., Schlicker D., Walrath K., Weiss V., Goldfine N. "MWM eddy current sensors for monitoring of crack initiation and growth during fatigue tests and in service," *International Journal of Fatigue*, 2001, Supplement: S477 – S485.

[8] Ball, D., Sigl, K., McKeighan, P., Veit, A.., Grundy, D., Washabaugh, A., Goldfine, N., "An Experimental and Analytical Investigation of Multi-Site Damage in Mechanically Fastened Joints," USAF Aircraft Structural Integrity Program (ASIP) Conference, Memphis, TN, December 2004.

[9] Zilberstein, V., Fisher, M., Grundy, D., Schlicker, D., Tsukernik, V., Vengrinovich, V., Goldfine, N. "Residual and applied stress estimation from directional magnetic permeability measurements with MWM sensors," *Journal of Pressure Vessel Technology*, August 2002: Volume 124, 375-381.

[10] Suits, M., NASA Shuttle NDE Panel Discussion: "Main Propulsion System (MPS) LOX and LH2 Feedline Flowliner Inspection," ASNT Fall Conference and Quality Testing Show, Las Vegas, NV, November 2004.

[11] ASTM E606-92 (1998) "Standard Practice for Strain-Controlled Fatigue Testing," *Annual Book of ASTM Standards*, Section Three, Vol. 3.01, pp. 580-594, 2003, ASTM International.

[12] Goldfine, N., Zilberstein, V., Schlicker, D., Sheiretov, Y., Walrath, K., Washabaugh, A., Van Otterloo, D., "Surface Mounted Periodic Field Current Sensors for Structural Health Monitoring," SPIE, Smart Structures and Materials NDE for Health Monitoring and Diagnostics, Newport Beach, California; March 2001.

[13] Shay, I., V. Zilberstein, A. Washabaugh, N. Goldfine, "Remote Temperature and Stress Monitoring Using Low Frequency Inductive Sensing," SPIE NDE/Health Monitoring of Aerospace Materials and Composites, San Diego, CA, 2003.

